Compact Modeling of Bistable Electrostatic Actuators

J. Xu, R. B. Darling, and P. O. Lauritzen

Dept. of Electrical Engineering, Box 352500
University of Washington, Seattle, WA, USA, bdarling@ee.washington.edu

ABSTRACT

A compact circuit simulation model for a bistable electrostatic cantilever actuator is presented which is appropriate for circuit and system simulation of RF MEMS switches. This simplified model captures the essential physical features of a cantilever, including hysteresis and bistability, making it suitable for large-signal circuit analyses. The model is extremely compact by means of using only a single internal system variable and requires only a small number of material and geometrical parameters. The model also properly conserves charge while still representing a voltage-variable, bistable capacitance.

Keywords: bistability, cantilevers, compact modeling, electrostatic actuators, MEMS switches.

INTRODUCTION

Electrostatic actuators are a popular, low-power means for achieving movement in microelectromechanical systems (MEMS). These may be fabricated as singly or multiply supported deformable beams or membranes, utilizing metal, polysilicon, or elastomer thin films over a sacrificial layer which is etched away to form the air gap. The geometry of a singly supported cantilever actuator is shown in Fig. 1. This consists of a prismatic beam of dimensions $W \times L \times d_0$ which is supported on a post above an air gap of h_0, with free space permittivity ε_0, and a landing dielectric layer of thickness d_1 with a permittivity of ε_1.

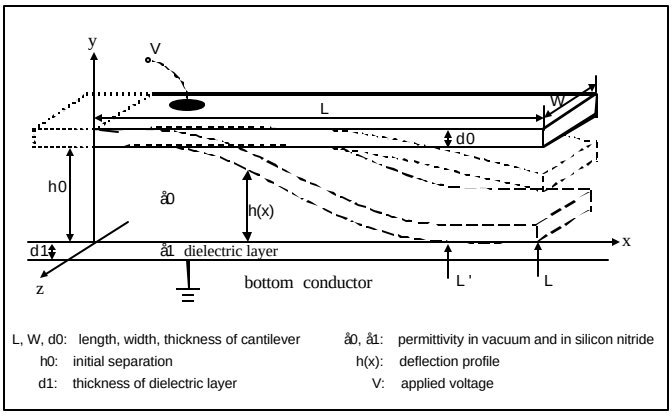

Figure 1. Geometry of cantilever.

As an external voltage is applied to the cantilever, electrostatic attraction forces pull the tip downward. This deforms the cantilever into a deflection profile h(x) as shown. Past a certain point, typically about one-third of the air gap spacing at the tip, the balance of forces becomes unstable and the tip snaps all the way down. In this structure, a dielectric spacer layer is used to avoid short circuiting the actuation voltage when the cantilever tip deflects fully downward. Increasing the applied voltage causes additional bending of the cantilever as it rolls out along the bottom dielectric landing layer. The applied voltage must be reduced from the snap down value before the tip will spring back up, reflecting the hysteresis that is inherent to bistable systems. This physical behavior produces a bistable voltage-variable capacitance which has many applications in RF switching [1,2].

Various analytical approaches have been presented for describing the deflection characteristics of electrostatic actuators, but these have so far been limited to the regime of small deflections and have not lent themselves to compact simulation models. Petersen's analytical model for a simple, singly supported cantilever remains the most cited model, but this applies only to deflections up to the snap-down point [3]. Thus far, no analytical models have been reported for treating the large deflection case where the cantilever has fully contacted the bottom surface. Such models are necessary for circuit simulations which involve electrostatic actuators used as capacitive RF switches. The strong nonlinearity and bistable capacitance characteristics require special considerations in model construction.

SIMPLIFIED CANTILEVER GEOMETRY

Our modeling approach is based upon a very simple sectional model of the cantilevered beam which is described by a single system variable α which represents the angular deflection of a rigid section about the support point at x = 0. Past the point where the tip has contacted the landing layer, the rigid section is divided into two, with the section between L' and L lying flat against the landing layer. The simplified deflection profiles which are associated with the system variable α are shown in Fig. 2, along with more accurate Matlab simulations which show the error of this sectional rigid body approximation. This simplified geometry describes two distinct cases of $\alpha < \alpha_T$ and $\alpha > \alpha_T$, where the deflection angle associated with the tip just touching the landing layer at x = L is $\alpha_T = \tan^{-1}(h_0/L)$. This

choice allows a single system variable to simultaneously and smoothly treat the two cases of the small and large (touching) deflections. Other choices of system variables which might involve the tip deflection h(L) or the contacting edge L' would only work over one of the two cases and would require substantially more model complexity. A far more compact device model results than one using a complete system function such as h(x) to represent the internal state of the system.

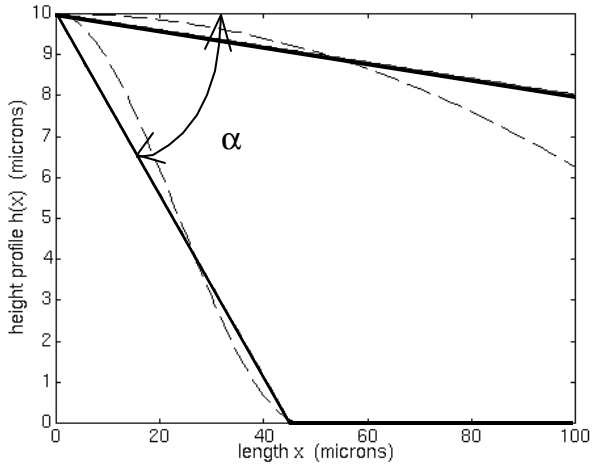

Figure 2. Simplified deflection profiles for both stable states at 150 Volts (thick lines). Dashed profiles are a Matlab solution to the electromechanical equations.

MODEL EQUATIONS

Static equilibrium is achieved in the cantilever by equating the mechanical restoring torque τ_m to the electrostatic deflecting torque τ_e, where both are nonlinear functions of the deflection angle α.

For case 1 where $\alpha < \alpha_T$, the mechanical restoring torque is simplified to an angular spring constant k_m, which can be estimated from the small deflection limit, $k_m = L^2F(L)/(h_0 - h(L))$. For case 2 where $\alpha > \alpha_T$, the cantilever contains two bends of equal angle α, so the effective angular spring constant is doubled in this region of operation. The two cases are connected by a smoothing function to produce

$$\boldsymbol{t}_m = k_m \boldsymbol{a} \frac{1+2e^{l(a-a_T)}}{1+e^{l(a-a_T)}} \quad , \tag{1}$$

where λ is a parameter characterizing the softness of the tip deformation at contact. Typically, $\lambda = 20$ for α in radians.

The electrostatic deflection torque is calculated from Gauss' Law and the simplified cantilever geometry with a voltage V applied between the cantilever and the landing electrode. The deflection profile is given by

$$h(x) = \max\begin{cases} h_0 - x\tan\boldsymbol{a} \\ 0 \end{cases} \quad . \tag{2}$$

Neglecting fringe fields, this gives rise to a y-directed electric field of

$$E_y(x) = \frac{\dfrac{V}{\boldsymbol{e}_0}}{\dfrac{d_1}{\boldsymbol{e}_1} + \dfrac{h(x)}{\boldsymbol{e}_0}} \quad . \tag{3}$$

The charge per unit length of the cantilever is then

$$Q'(x) = W\boldsymbol{e}_o E_y(x) \quad . \tag{4}$$

The electrostatic deflection torque and the total charge on the cantilever can then be computed as integrals of (3) and (4):

$$\boldsymbol{t}_e = \int_0^L Q'(x)\, E_y(x)\, x\, dx \quad , \tag{5}$$

$$Q = \int_0^L Q'(x)\, dx \quad . \tag{6}$$

Both of the above integrals can be performed in closed form as a function of the system variable α to smoothly treat both cases 1 and 2.

The dynamics of the cantilever are included into the model by calculating the electric current as the time derivative of the stored charge,

$$i(t) = \frac{dQ}{dt} \quad . \tag{7}$$

Mechanical damping is included to aid numerical convergence. The damping produces a transient difference between the electrostatic and mechanical torques,

$$\boldsymbol{t}_e = \boldsymbol{t}_m + D_a \frac{d\boldsymbol{a}}{dt} \quad , \tag{8}$$

where D_a is the angular damping coefficient.

BISTABLE DC SOLUTIONS

The system variable α is iterated during the simulation to produce a solution to Eq. (8). The voltage which is associated with a given angle of deflection α is determined by equating the electrostatic deflection torque to the mechanical restoring torque, $\tau_e = \tau_m$. Depending upon the applied voltage, one or three solution points exist, as

shown in Figs. 3(a,b) which plot τ_e and τ_m versus α. When three solution points exist, only two will be stable in steady-state, giving rise to the bistability found in these structures. As shown in Figs. 3(a,b), the functions τ_e and τ_m are both smooth and well behaved functions over the full range of α, leading to a device model which does not incur jumps or convergence problems at any operating point, including the touch down and release of the cantilever.

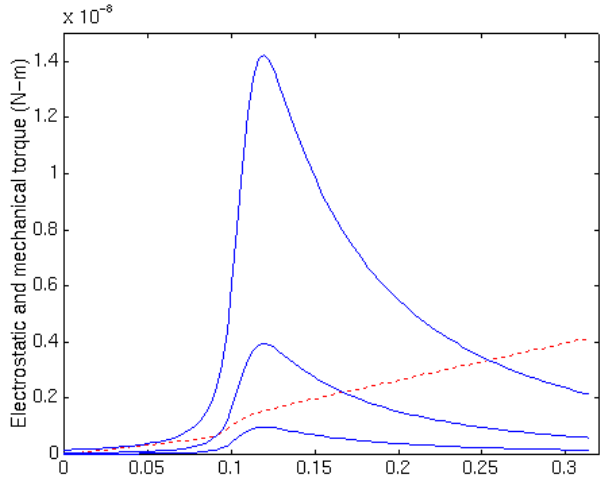

(a)

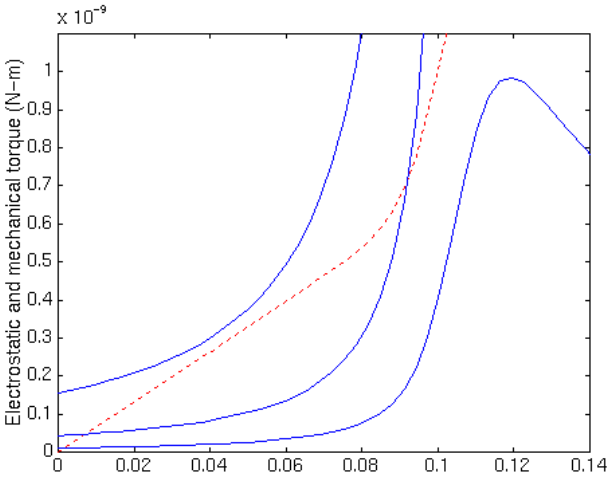

(b)

Figure 3. Electrostatic deflection torque (solid) and mechanical restoring torque (dashed) versus deflection angle α in radians for an applied 50 V, 100 V, and 190 V. Fig. 3(b) is an expansion of the origin region of Fig. 3(a).

The capacitance-voltage characteristics of the cantilever can be computed from the simplified deflection profile as

$$C(V) = \int_0^L \frac{W\, dx}{\frac{d_1}{e_1} + \frac{h(x)}{e_0}} \quad . \tag{9}$$

These are shown in Fig. 4 for the compact model and for a more exact deflection profile computed using Matlab. Relatively good agreement is obtained in the snap-down and spring-up voltages, and in the closed-state capacitance of around 80-100 fF. It is important to note that the capacitance of this structure as computed using Eq. (9) represents the small-signal AC capacitance that would be present for RF frequencies. This is quite different from the large-signal capacitance calculated as dQ/dV.

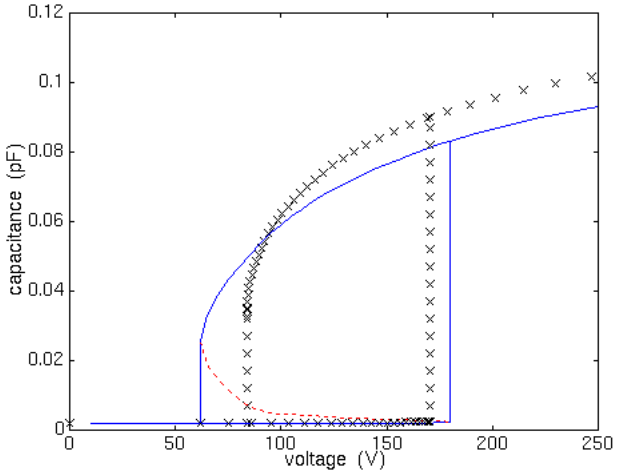

Figure 4. Capacitance-voltage characteristics of compact model (solid) and from a Matlab solution (crosses).

SIMULATION RESULTS

The model equations were implemented in MAST HDL for simulation with the Saber simulator. Of particular interest are the electrical characteristics of this switch in response to an applied voltage pulse. The nonlinear and bistable capacitance creates unusual current waveforms that change abruptly during the snap-down and spring-up phases of operation. When the cantilever is snapped down, the capacitance is nearly a hundred-fold larger than when it is up and this large, abrupt increase in capacitance causes the supply current to increase drastically during the closure phase. A similarly large current also flows during the initial part of the release phase.

The Saber simulator was used to sweep the applied voltage in a ramped pulse of 200 V peak with rise, fall, and high times of 5 µs. This was applied to the compact model through a 10 Ω series resistor. The internal system variable α is plotted versus voltage in Fig. 5. This smooth characteristic properly displays the bistability and hysteresis in the device using only the single system variable of α. The snap-down and spring-up voltages of Fig. 5 differ from those of Fig. 4 only because of slight differences in the implementation of the smoothing functions. Thus, this provides a very compact analytical model for the cantilever, extending the previous work of Petersen to the case of large

Proc. Transducers'97, vol. 2, pp. 1165-1168, Chicago, IL, 1997.

[3] K. E. Petersen, "Dynamic Micromechanics on Silicon: Techniques and Devices," IEEE Trans. Electron Dev., vol. ED-25, no. 10, pp. 1241-1250, Oct. 1978.

[4] J. R. Gilbert, G. K. Ananthasuresh, and S. D. Senturia, "3D Modeling of Contact Problems and Hysteresis in Coupled Electro-Mechanics," Proc. MEMS 1996, pp. 127-132, San Diego, CA, 1996.

ACKNOWLEDGEMENTS

This work was supported by the NSF Center for the Design of Analog/Digital Integrated Circuits (CDADIC).